



HAL
open science

Selective inhibition of ADAM12 catalytic activity through engineering of tissue inhibitor of metalloproteinases (TIMP)-2

Marie Kveiborg, Jonas Jacobsen, Meng-Huee Lee, Hideaki Nagase, Ulla M Wewer, Gillian Murphy

► **To cite this version:**

Marie Kveiborg, Jonas Jacobsen, Meng-Huee Lee, Hideaki Nagase, Ulla M Wewer, et al.. Selective inhibition of ADAM12 catalytic activity through engineering of tissue inhibitor of metalloproteinases (TIMP)-2. *Biochemical Journal*, 2010, 430 (1), pp.79-86. 10.1042/BJ20100649 . hal-00506526

HAL Id: hal-00506526

<https://hal.science/hal-00506526>

Submitted on 28 Jul 2010

HAL is a multi-disciplinary open access archive for the deposit and dissemination of scientific research documents, whether they are published or not. The documents may come from teaching and research institutions in France or abroad, or from public or private research centers.

L'archive ouverte pluridisciplinaire **HAL**, est destinée au dépôt et à la diffusion de documents scientifiques de niveau recherche, publiés ou non, émanant des établissements d'enseignement et de recherche français ou étrangers, des laboratoires publics ou privés.

Selective inhibition of ADAM12 catalytic activity through engineering of tissue inhibitor of metalloproteinases (TIMP)-2

Marie Kveiborg^{*,§}, Jonas Jacobsen^{*,§}, Meng-Huee Lee[†], Hideaki Nagase[‡], Ulla M. Wewer^{*,¶}, and Gillian Murphy^{†,¶}

^{*}Department of Biomedical Sciences and Biotech Research and Innovation Centre (BRIC), University of Copenhagen, Ole Maaløes Vej 5, 2200 Copenhagen, Denmark

[†]Department of Oncology, Cambridge University, Cancer Research Institute, Li Ka Shing Centre, Cambridge CB2 0RE, UK

[‡]Kennedy Institute of Rheumatology Division, Faculty of Medicine, Imperial College London, 65 Aspenlea Road, London W6 8LH, UK

^{§,¶}These authors contributed equally to the study.

Short title: Selective inhibition of ADAM12 by TIMP engineering

Keywords: ADAM12; TIMPs; TACE; ectodomain shedding; therapeutic target

Corresponding author: Gillian Murphy, Dept of Oncology, Cambridge University, Cancer Research Institute, Li Ka Shing Centre, Robinson Way, Cambridge CB2 0RE, UK
Phone: +44 (0)1223 404470; Fax: +44 (0)1223 404573; Email: gm290@cam.ac.uk

¹Abbreviations used: ADAM, a disintegrin and metalloprotease; AP, alkaline phosphatase; Cm-Tf, S-carboxymethylated transferrin; EGF, epidermal growth factor; EGFR, epidermal growth factor receptor; HB-EGF, heparin-binding epidermal growth factor; LRP-1, low density lipoprotein receptor-related protein-1; MMP, matrix metalloproteinase; MT-MMP, membrane-type matrix metalloproteinase; SFM, serum-free medium; TACE, tumour necrosis factor alpha converting enzyme; TIMP, tissue inhibitor of metalloproteinases.

Accepted Manuscript

SYNOPSIS

The disintegrin and metalloprotease ADAM12 has important functions in normal physiology as well as in diseases, such as cancer. Little is known about how ADAM12 confers its protumorigenic effect; however, its proteolytic capacity is likely a key component. Thus, selective inhibition of ADAM12 activity may be of great value therapeutically and as an investigative tool to elucidate its mechanisms of actions. We have previously reported the inhibitory profile of tissue inhibitors of metalloproteinases (TIMPs) against ADAM12, demonstrating in addition to TIMP-3, a unique ADAM inhibitory activity of TIMP-2. These findings strongly suggest that it is feasible to design a TIMP mutant selectively inhibiting ADAM12. With this purpose, we characterized the molecular determinants of the ADAM12–TIMP complex formation as compared with known molecular requirements for TIMP-mediated inhibition of ADAM17/TACE. Kinetic analysis using a fluorescent-peptide substrate demonstrated that the molecular interactions of N-terminal domains of TIMPs (N-TIMPs) with ADAM12 and TACE are for the most part comparable, yet revealed striking unique features of TIMP-mediated ADAM12 inhibition. Intriguingly, we found that removal of the AB-loop in N-TIMP-2, which is known to impair its interaction with TACE, resulted in increased affinity to ADAM12. Importantly, using a cell-based epidermal growth factor-shedding assay, we demonstrated for the first time an inhibitory activity of TIMPs against the transmembrane ADAM12-L, verifying the distinctive inhibitory abilities of N-TIMP-2 and engineered N-TIMP-2 mutants in a cellular environment. Together, our findings support the idea that a distinctive ADAM12 inhibitor with future therapeutic potential can be designed.

THIS IS NOT THE VERSION OF RECORD - see doi:10.1042/BJ20100649

Accepted Manuscript

INTRODUCTION

ADAM12, a disintegrin and metalloprotease also known as meltrin α , is a multifunctional zinc-dependent enzyme and one of 13 catalytically active human ADAMs [1]. In humans, ADAM12 is expressed as a classical type 1 transmembrane form (ADAM12-L) and as a shorter secreted splice variant (ADAM12-S). Both forms consist of a pro domain, a catalytic domain, and cell-adhesive disintegrin, cysteine-rich, and epidermal growth factor (EGF)-like domains, but ADAM12-S lacks the C-terminal transmembrane and cytoplasmic domains found in ADAM12-L [2]. A key feature of the ADAMs, including ADAM12, is their ability to “shed” membrane-anchored proteins and thus regulate the availability of bioreactive molecules, such as cell-surface receptors, growth factors, and cytokines [3, 4]. Previous *in vitro* studies have implicated ADAM12-L in ectodomain shedding of several epidermal growth factor receptor (EGFR) ligands (EGF, heparin-binding EGF (HB-EGF), and betacellulin) [5, 6], the Notch ligand Delta-like 1 [7], and oxytocinase [8], whereas ADAM12-S can cleave insulin-like growth factor binding protein-3 and -5 [9]. Whether cleavage of these substrates represents physiologically significant functions remains to be shown. However, ADAM12 appears to play an important pathogenic role in diseases such as osteoarthritis, cardiac hypertrophy, and several human cancers [1], thus arguing in favour of selectively targeting its protease activity in efforts to design potential new therapies [10].

Known endogenous regulators of ADAM protease functions include certain members of the family of tissue inhibitors of metalloproteinases (TIMPs), which are mainly known for their inhibitory activity against the matrix metalloproteinases (MMPs). Four homologous human TIMPs (TIMP-1, TIMP-2, TIMP-3, and TIMP-4) have been characterized, with all inhibiting metalloproteinases in a 1:1 stoichiometry by tightly binding to the active site of the enzymes. Structural analyses have revealed that the ~24 kDa TIMPs are composed of two very distinct N- and C-terminal domains, of which the N-terminal domain is responsible for most contact made with the active site of the enzyme [11, 12]. The majority of MMPs are well inhibited by all TIMPs, except that TIMP-1 exhibits little activity toward membrane-type MMPs (MT-MMPs). Apart from TIMP-1, which is a good inhibitor of ADAM10 [13], TIMP-3 has been considered the sole endogenous ADAM modulator. Based on a series of mutagenesis studies, as well as the high-resolution cocrystal structure of N-TIMP-3 in complex with ADAM17/TACE (tumour necrosis factor alpha converting enzyme), the TIMP reactive ridge has been localized to the N-terminal wedge, the AB-loop, and the CD- and EF-connecting loops of the molecule (Fig. 1) [12, 14].

Due to the high structural similarities of their catalytic domains, metalloproteinases—including the ADAMs—are notoriously difficult to target selectively [15, 16]. However, we recently discovered that TIMP-2 exhibits high inhibitory activity against ADAM12 ($K_{i(\text{app})} = 44 \text{ nM}$) [17]. This apparently unique TIMP inhibitory profile observed for ADAM12 (TIMP-3 > TIMP-2 >> TIMP-1) indicates that the engineering of an ADAM12-selective TIMP mutant should be possible. With this as our goal, in this study we mapped and characterized the molecular determinants involved in ADAM12–TIMP complex formation. Using a quenched fluorescent-peptide assay, we examined the inhibitory activity of wild-type and mutant forms of TIMPs and N-TIMPs against recombinant full-length ADAM12-S and truncated ADAM12-Cat, consisting of the pro and catalytic domains. By comparing our findings with the inhibitory profile of TIMPs against TACE, we demonstrated that, while the molecular interactions of TIMPs with ADAM12 and TACE are largely comparable, certain unique features of the ADAM12–TIMP interaction exist. Most remarkably, we found that removal of the AB-loop in N-TIMP-2, which significantly impairs its interaction with TACE, increased its affinity to ADAM12. Importantly, these *in vitro* data were confirmed in cell-based shedding assays using membrane-anchored EGF and HB-EGF as the cellular substrates and native ADAM proteases. Thus, the reported results clearly encourage further

efforts to develop a selective ADAM12 inhibitor that may have potential future experimental and/or therapeutic applications.

EXPERIMENTAL

Chemicals

Unless otherwise stated, all reagents and chemicals were from Sigma-Aldrich. Fluorescent-peptide substrates, Dabcyl-LAQAhomoPheRSK(FAM)-NH₂ (hydrolysed by ADAMs) and Dabcyl-GPLGMRGK(FAM)-NH₂ (hydrolysed by MMPs) were purchased from BioZyme Incorporated. The TACE inhibitor TAPI-2 and phorbol-12-myristate-13-acetate (PMA) were from Calbiochem.

Plasmids

The mammalian expression vector pCEP-4 and the *Escherichia coli* expression vector pRSET-C were from Invitrogen. Wild-type and catalytically inactive (E351Q point mutation) full-length human ADAM12-L constructs in the pcDNA3.1 vector were previously described [18, 19]. The cDNA constructs encoding pro-EGF or pro-HB-EGF fused to alkaline phosphatase (AP) in the pRC/CMV expression vector (AP-EGF and AP-HB-EGF) were kindly provided by Dr. Shigeki Higashiyama, Ehime University Graduate School of Medicine, Ehime, Japan and Dr. Michael Freeman, Children's Hospital Boston, MA, USA, respectively.

Production of recombinant proteins

Human ADAM12 cDNAs (NM_021641) encoding either full-length ADAM12-S (amino acids 1-707) or the ADAM12 pro and catalytic domains (ADAM12-Cat, amino acids 1-419) in the pCEP4 plasmid were expressed in HEK-293 EBNA cells and recombinant proteins were purified as previously described [17, 20]. Human MMP-1, MMP-2, MMP-3, and MT1-MMP were expressed in *E. coli*, purified, and the active site titrated as described [21, 22]. Recombinant ADAM17 ectodomain (TACE651; TACE-long), was expressed from baculovirus (a kind gift of Dr. David Becherer, GlaxoSmithKline) and purified by Dr. Peter Stanley according to the method of Milla et al. [23], with minor modifications. The mature catalytic domain of ADAM17 (TACE477GHHis₆; TACE-Cat) was also prepared using the baculovirus system and was the generous gift of Dr. Becherer. Expression and purification of human full-length TIMP-1 and TIMP-2, as well as the N-terminal domain of TIMP-3 (N-TIMP-3), were all as previously described [24-26]. N-TIMP-1 and N-TIMP-2 in the pRSET-C *E. coli* expression vector and all variants of these (N-TIMP-1^{TACE}, N-TIMP-1[V4S], N-TIMP-1[V4A], N-TIMP-1[T98L], N-TIMP-1[TIMP-2-ABloop], N-TIMP-1[TIMP-3-ABloop], N-TIMP-2^{TACE}, N-TIMP-2^{TACE}[L100E], N-TIMP-2-ΔABloop, and N-TIMP-2^{TACE}[F34G]) were generated as previously reported [14, 27, 28] and transformed into *E. coli* BL21(DE3). Cells were grown in LB media containing 50 µg/ml carbenicillin until OD 600 = 0.8, then protein expression was induced by adding 1 mM isopropyl-beta-D-thiogalactopyranoside followed by cultivation for 4 h at 37 °C. Cells were harvested by centrifugation, resuspended in 50 mM Tris-HCl pH 8.0, and lysed by sonication (MSE Soniprep 150). Inclusion bodies were collected by centrifugation for 15 min and washed once in 50 mM Tris-HCl pH 8.0 containing 150 mM NaCl, twice in water, once in 2-propanol, and once in water, then resuspended in inclusion body buffer containing 5 M guanidine hydrochloride, 50 mM Tris-HCl pH 8.0, 0.2 mM GSH (reduced), 0.8 mM GSSG (oxidized), and 500 mM NaCl. Resuspended inclusion bodies were *in vitro* refolded essentially as previously described [27-29]. All proteins were purified by Ni-NTA and cation exchange chromatography and finally dialysed into 25 mM Hepes containing 100 mM NaCl, 0.05% Brij35, and 0.02% sodium azide. To determine the concentration of active N-TIMPs in each preparation, the inhibitor was titrated against a known amount of either MMP-1 or MMP-2. In addition to the active-site titrations, proteins were analysed by reducing and nonreducing SDS-

PAGE on 15% polyacrylamide gels followed by staining with Coomassie Brilliant Blue R-250. Single bands shifting in mobility under reduced and nonreduced conditions indicated that correct folding had occurred.

Kinetic analysis

Apparent inhibition constants ($K_{i(\text{app})}$) were measured using a fluorescent-peptide assay [30]. In brief, 5 μl of recombinant human ADAM12-Cat (0.1 nM final concentration) or full-length ADAM12-S (0.25 nM final concentration) was mixed with 5 μl of TIMPs at various concentrations and 90 μl 20 mM Tris-HCl pH 8.0 containing 20 mM NaCl, 1 mM CaCl_2 , and 0.05% Brij35 and preincubated for 2 h at 37 °C. Reactions were initiated by adding 5 μl of the quenched fluorescent-peptide substrate (10 μM final concentration) and steady-state velocities (V_s) were monitored on a BMG Fluorostar Optima fluorometer (excitation at 485 nM and emission at 530 nM). To determine $K_{i(\text{app})}$ values, V_s was plotted against TIMP concentration and data were fitted to the Morrison equation describing tight-binding inhibition using the computer software Graph Pad Prism 5.0 (Graph Pad Software) [17, 30, 31].

Cell culture

Human 293-VnR cells were kindly provided by Dr. Archana Sanjay, Temple University School of Medicine, Philadelphia PA, USA and cultured in Dulbecco's modified Eagle medium supplemented with 10% fetal bovine serum, 1% L-glutamine, and 1% penicillin/streptomycin (Invitrogen) as previously described [18]. The cells were transiently transfected with AP-EGF together with wild-type ADAM12-L or ADAM12-L (E351Q) using FuGENE® 6 Transfection Reagent (Roche Diagnostics) according to the manufacturer's description. Human HT1080 cells (from American Type Culture Collection) were cultured and transfected with the AP-HB-EGF construct as described above. Forty-eight hours after transfection, cells were trypsinized, then stained for cell-surface alkaline phosphatase expression using the mouse monoclonal anti-alkaline phosphatase (clone 8B6) ascites fluid (Sigma-Aldrich) and Alexa Fluor® 488-donkey anti-mouse IgG (Invitrogen). The 10% highest-expressing cells were isolated by FACS and maintained in culture by selection with 500 $\mu\text{g}/\text{ml}$ geneticin (G418, Invitrogen).

Shedding assays

ADAM12-mediated AP-EGF shedding was determined by cotransfection of 293-VnR cells with either wild-type or catalytically inactive (E351Q) full-length ADAM12-L together with AP-EGF as previously described [18]. Twenty-four hours after transfection, cells were seeded into 24-well plates and the following day washed twice with serum-free medium (SFM), treated with recombinant TIMP inhibitors or vehicle control as indicated for an initial 15 min, then incubated for 1 h with 250 μl fresh SFM with or without inhibitor. For photometric quantitation of AP-EGF shedding, cell-conditioned medium was harvested and the cell layer lysed in 250 μl 1% Triton X-100 in PBS. Conditioned SFM or cell lysate (50 μl) was mixed with 50 μl of a 2 mg/ml solution of the alkaline phosphatase substrate 4-nitrophenyl and each well assayed in duplicate in a 96-well plate. After incubation at 37 °C for 1-2 h, the amount of product was quantified by measuring the absorbance at 405 nm. All treatments were performed in triplicate. AP-EGF shedding in cells transfected with wild-type or catalytically inactive ADAM12 was calculated as alkaline phosphatase activity in the conditioned media divided by alkaline phosphatase activity in the media and corresponding cell lysate after subtracting the background signal from nontransfected cells. The value obtained for wild-type ADAM12-L was then divided by the value for catalytically inactive ADAM12-L (E351Q), and the ADAM12-mediated cleavage calculated as the percentage of that observed in control-treated cells. To ensure equal expression levels of wild-type and catalytically

inactive ADAM12-L, cell lysates from triplicate wells were pooled and examined by SDS-PAGE and Western blot as described [18, 19].

As a measurement of TACE-mediated shedding, HT1080 cells stably expressing AP-HB-EGF were seeded in 96-well plates, then the confluent cell layer was treated 24 h later with 400 nM PMA or vehicle control for 30 min, and alkaline phosphatase activity was measured in quadruplicate as described above. All data were analysed by one-way analysis of variance with Dunnett's or Bonferroni's post tests for multiple comparisons, with $p < 0.05$ considered statistically significant.

RESULTS AND DISCUSSION

Non-catalytic domains of ADAM12 regulate the binding affinity to TIMP-2 and-3

Together, the four TIMP inhibitors regulate the activity of all catalytically active ADAMs, a disintegrin and metalloproteases with thrombospondin type 1 repeats (ADAMTSs), and MMPs, which share high structural similarity in their catalytic domains [32]. Apart from a few exceptions, soluble MMPs are inhibited by TIMP-1–4, transmembrane MT-MMPs by TIMP-2–4, and ADAMs and ADAMTSs by TIMP-3. However, we recently demonstrated that in contrast to other ADAMs, ADAM12 is also inhibited by TIMP-2 [17]. In that earlier study, the inhibitory activities of TIMP-1–3 were evaluated using the general substrate S-carboxymethylated transferrin (Cm-Tf), which at the time of the study was the only feasible substrate for kinetic analysis of ADAM12. Cm-Tf is in some ways a suboptimal substrate, as it generates degradation products that undergo further processing. Thus, in the present study we utilized a novel quenched fluorescent-peptide assay to examine the apparent binding constants ($K_{i(\text{app})}$) of wild-type and mutant forms of TIMPs and N-TIMPs against ADAM12-S (Table I). Because our previous data revealed that the noncatalytic C-terminal domains of ADAM12-S regulate the catalytic activity, we tested various inhibitors against both full-length wild-type ADAM12-S and the truncated ADAM12-Cat that consists of the pro and catalytic domains. The $K_{i(\text{app})}$ values produced corresponded very well with our previous results using Cm-Tf as a substrate [17], supporting the use of Cm-Tf as a reliable substrate for kinetic studies.

N-TIMP-3 was the most active inhibitor of both ADAM12-S ($K_{i(\text{app})} = 4.4$ nM) and ADAM12-Cat ($K_{i(\text{app})} = 0.93$ nM) (Table I). The kinetic analysis further revealed that the inhibitory activity of N-TIMP-2 ($K_{i(\text{app})} = 5.5$ nM) and TIMP-2 ($K_{i(\text{app})} = 2.5$ nM) against ADAM12-Cat greatly surpassed that of N-TIMP-2 ($K_{i(\text{app})} = 69.7$ nM) and TIMP-2 ($K_{i(\text{app})} = 84.0$ nM) against full-length ADAM12-S. As expected, N-TIMP-1 and TIMP-1 were the poorest inhibitors of ADAM12 activities, with $K_{i(\text{app})}$ values in the 0.2–0.8 μM range. Based on these data, the N-terminal domains of TIMP-2 and TIMP-3 appear to be sufficient for the inhibition of ADAM12-S. In addition, as previously demonstrated and in agreement with what has been previously shown for TACE [30], deletion of the C-terminal disintegrin and cysteine-rich domains in ADAM12 strengthened the inhibitory activity, which is most dramatically seen for TIMP-2 (34-fold, Table I).

As revealed by the cocrystal structure of the TACE–N-TIMP-3 complex, as well as earlier mutagenesis studies, the TIMP reactive ridge is located exclusively in the N-terminal domain (Fig. 1 and [12, 14]). However, the C-terminal domains of both the inhibitor and the enzyme have been shown to regulate the affinity of the complex formation between ADAMs and TIMPs [33, 34]. Model docking experiments of snake venom metalloproteinases VAP-1 and -2 with N-TIMP-3 suggest that the cysteine-rich domain approaches the active-site cleft, potentially interfering with the bound TIMP inhibitor [12]. Thus, our findings may be explained by steric clashes between TIMPs and the cysteine-rich domains. In contrast to our findings, the N-terminal domains of TIMP-1 and TIMP-3 have been reported to be insufficient for the inhibition of ADAM10 [34], indicating the presence of yet unmapped interaction sites in TIMP-1 and TIMP-3 outside the catalytic cleft.

N-TIMP mutagenesis studies

As mentioned above, previous detailed mutagenesis studies have addressed the inactivity of TIMP-1, -2, and -4 against TACE [27, 28, 35]. Thus, we used these findings, together with sequence alignments supported by the cocrystal structure of TACE–N-TIMP-3 (Fig. 1 and [12]) to predict a number of ADAM12-interacting sites located in the TIMP reactive ridge. Interaction sites that were found to be identical in TIMP-2 and TIMP-3, but substituted in the weaker inhibitor TIMP-1, were selected and examined. Specifically, we hypothesized that a polar residue in position 4, as well as a leucine in the EF-loop (position 94 in N-TIMP-3), would be critical for binding to ADAM12. In addition, we chose to investigate the contribution of the highly variable AB-loops to binding, because the AB-loop region of TIMP-3 has proved to be critical for the interaction with TACE [28, 29]. The previously reported N-TIMP mutants N-TIMP-1^{TACE} (V4S/V69L/T98L/TIMP-3–ABloop) [27] and N-TIMP-2^{TACE} (S2T/A70S/V71L/TIMP-3–ABloop) [28], both of which have high activity toward TACE, encompass affinity-optimizing mutations in all the regions we expected to be essential for potent inhibition of ADAM12. We therefore initiated our mutagenesis study by addressing if these TACE-directed mutants would also be improved in their reactivity toward ADAM12.

Indeed, both N-TIMP-1^{TACE} and N-TIMP-2^{TACE} proved to be excellent ADAM12 inhibitors, far exceeding the inhibitory potency of their wild-type counterparts (Table I). Compared with the wild-type forms, N-TIMP-1^{TACE} was improved more than 30-fold ($K_{i(\text{app})} = 16.4$ nM versus >500 nM) and N-TIMP-2^{TACE} showed a ~ 10 -fold enhancement ($K_{i(\text{app})} = 6.0$ nM versus 69.7 nM for ADAM12-S). The positive influence on binding of the TACE-directed mutants was even more pronounced for the interaction between ADAM12-Cat and N-TIMP-1^{TACE}, which displayed a >400 -fold increase when compared with wild-type N-TIMP-1. It is also noteworthy that N-TIMP-2^{TACE}, with a $K_{i(\text{app})}$ value of 0.65 nM for ADAM12-Cat, is the best ADAM12 inhibitor reported so far. The improved binding to ADAM12-S strongly suggests that our initial structural predictions were correct, and we next proceeded to dissect the contribution of the individual mutations to the binding affinity observed.

Adverse effects of N-TIMP-1 Val⁴ on ADAM12 interaction

The first six amino acids of TIMPs constitute the N-terminal reactive ridge that inserts into the primed site of the enzyme's catalytic cleft. The cocrystal structure of TACE–N-TIMP-3 demonstrated that the side chain of position 4 projects into the S3' pocket, and mutational analysis has indicated a preference for polar residues in this position [14]. When we compared the position 4 residues of TIMP-1, -2, and -3 (Fig. 1C), we noted that the serine found in TIMP-2 and TIMP-3 was substituted with a valine in the TIMP-1 sequence. Because this difference could indicate that ADAM12 prefers a polar residue in position 4, we tested the valine to serine mutant (N-TIMP-1[V4S]) to mimic the naturally occurring polar amino acid found in TIMP-2 and TIMP-3. This substitution resulted in a weakly improved binding affinity for ADAM12-S ($K_{i(\text{app})}$ of 122 nM versus >500 nM for wild-type N-TIMP-1) (Table I). Intriguingly, our kinetic analysis indicated that mutation to the less hydrophobic aliphatic alanine (V4A) was sufficient to overcome the unfavourable effects of valine ($K_{i(\text{app})} = 190$ nM).

The fact that mutation to the less hydrophobic alanine had almost the same improved binding capacity as the serine substitution contradicts previous TACE data, which showed that alanine decreased the affinity of N-TIMP-1 against TACE [14, 27]. The S3' pocket of TACE is a wide and relatively deep depression that is not filled by any of the naturally occurring residues (valine and serine) [36]. However, since the same scenario is true for ADAM12, where our

modelled structure of ADAM12 predicts an even deeper hydrophobic pocket with an 8.6 Å depression resembling that of TACE (data not shown), it does not explain the observed finding.

A leucine residue in the EF-loop is important for ADAM12 interaction

TIMP-2, and -3 contain a leucine residue in the EF-loop (Fig. 1C), and replacement of the corresponding threonine 98 on N-TIMP-1 with leucine (T98L) successfully transforms N-TIMP-1 into a potent tight binding inhibitor of both TACE and MT1-MMP [29]. To elucidate the impact of this particular leucine on the TIMP–ADAM12 interaction and to examine whether the T98L mutation in N-TIMP-1^{TACE} could be the key residue explaining the superior fold improvement of N-TIMP-1^{TACE} over N-TIMP-2^{TACE}, where a leucine in this position is naturally occurring, we examined the N-TIMP-1[T98L] mutant. As observed for other metalloproteinases otherwise insensitive to N-TIMP-1, the mutation of threonine 98 to leucine (T98L) transformed N-TIMP-1 into an active inhibitor of ADAM12-S and ADAM12-Cat ($K_{i(\text{app})} = 21.7$ nM and 11.2 nM, respectively) (Table I).

Previous studies have shown that the EF-loop leucine is a prerequisite for high-affinity inhibition of TACE to occur, because substitution of Leu¹⁰⁰ in N-TIMP-2^{TACE} with any existing amino acid led to poorer $K_{i(\text{app})}$ values [27]. To confirm this effect for ADAM12, we examined the inhibitory potency of the N-TIMP-2^{TACE}[L100E] mutant. Even though the L100E mutant showed reduced reactivity with ADAM12-S and ADAM12-Cat ($K_{i(\text{app})} = 22.0$ nM and 4.1 nM, respectively), the impairment was less pronounced than against TACE-Cat, where the mutation caused a ~24-fold decrease in the $K_{i(\text{app})}$ value (Table I and [29]). In the TACE–N-TIMP-3 cocrystal structure, the leucine protrudes from the EF-loop into a hydrophobic groove on TACE [12]; thus, the relatively mild impact of the L100E mutation could suggest compensatory electrostatic interactions of Glu¹⁰⁰ with sites in ADAM12.

N-TIMP-2 AB-loop deletion enhances the interaction with ADAM12

The AB-loop of TIMP-3 is of major importance for the inhibition of TACE [12]. It protrudes from the surface of the inhibitor and binds in a unique hydrophobic groove on TACE, with most direct intermolecular contacts being made *via* the phenyl group of phenylalanine at position 34 (Fig. 1A). Only TIMP-3 harbours a phenylalanine in this position, and kinetic studies have shown that TACE clearly favours the AB-loop of TIMP-3 over that of TIMP-2 [28]. To address the contribution of the AB-loop to ADAM12 binding, we first tested a N-TIMP-1 mutant whose short AB-loop (T³²T³³L³⁴Y³⁵) was replaced with either that of TIMP-2 (N³³D³⁴I³⁵Y³⁶G³⁷N³⁸P³⁹) or TIMP-3 (F³⁴G³⁵T³⁶). Whereas N-TIMP-1[TIMP-2–ABloop] remained a poor inhibitor of ADAM12-S, the binding capacity was improved 3-fold over that of N-TIMP-1 against ADAM12-Cat (Table I). Transfer of the AB-loop of TIMP-3 to N-TIMP-1 in the N-TIMP-1[TIMP-3–ABloop] mutant transformed the inhibitor into a high-affinity inhibitor of ADAM12-S with a $K_{i(\text{app})}$ of 66.0 nM (Table I). To explain the preference for the AB-loop of TIMP-3, we examined the importance of a phenylalanine at position 34. To this end, we used N-TIMP-2^{TACE} as a scaffold and mutated phenylalanine to glycine (F34G). With a $K_{i(\text{app})}$ value of 18.0 nM against ADAM12-S, the F34G mutant is weakly but substantially impaired in its binding to ADAM12-S compared with N-TIMP-2^{TACE} ($K_{i(\text{app})} = 6.0$ nM) (Table I). As a final experiment designed to investigate the role of the AB-loop in the interaction between ADAM12 and TIMPs, we evaluated an N-TIMP-2– Δ ABloop mutant. In this mutant, the AB-loop region of TIMP-2 (N³³D³⁴I³⁵Y³⁶G³⁷N³⁸P³⁹) was completely deleted. Inexplicably, the Δ ABloop mutant showed a 2–3-fold increase in affinity against ADAM12-S ($K_{i(\text{app})} = 28.1$ nM) and ADAM12-Cat ($K_{i(\text{app})} = 2.5$ nM) (Table I), which is in direct contrast to the interaction with TACE and MT1-MMP, where removal of the AB-loop of N-TIMP-2 was shown to have radical negative consequences [14, 22].

These findings, together with the fact that ADAM12, unlike TACE, is well inhibited by wild-type TIMP-2, suggest major differences in their interactions with the AB-loop. In the TACE–N-TIMP-3 cocrystal structure, the phenyl group of phenylalanine at position 34 in the AB-loop makes a number of direct contacts with a unique hydrophobic groove on the surface of TACE formed by the side chains of Tyr³⁵², Val³⁵³, Tyr³⁶⁹, and Leu³⁸⁰. In the region between sIV and sV (Fig. 1B), the sequence divergence between ADAM12 and ADAM17 is very large, indicating that the hydrophobic pocket accommodating Phe³⁴ is a unique structural feature of TACE. Therefore, the structural delineation of ADAM12–N-TIMP-3 is required to explain exactly why the F34G mutation decreases the $K_{i(\text{app})}$ value of N-TIMP-2^{TACE} approximately 3-fold.

To validate these unexpected findings that N-TIMP-2– Δ ABloop showed a ~2.5-fold increase in its affinity toward ADAM12 when compared with N-TIMP-2 wild-type, we reassessed previously determined $K_{i(\text{app})}$ values for this mutant against a number of soluble and membrane-type MMPs (MMP1, MMP2, MMP3, and MT1-MMP). These studies confirmed the values already provided in the literature, demonstrating that deletion of the AB-loop of TIMP-2 has little impact on the interaction with soluble MMPs, but is detrimental to the interaction with cell surface-bound metalloproteinases (data not shown). Hence, the exception to this rule appears to be ADAM12, and consequently N-TIMP-2– Δ ABloop appears to be a selective inhibitor of ADAM12.

TIMPs are functional inhibitors of ADAM12-mediated EGF-shedding

The *in vitro*-established unique inhibitory profile for ADAM12 may offer a possibility to exploit TIMPs to discover hitherto unknown ADAM12-mediated cell-surface shedding events. We therefore used a cell-based shedding assay to examine whether the findings from our kinetic studies of soluble ADAM12-S reflected TIMP inhibition of the transmembrane ADAM12-L. For this purpose, a pro-EGF-alkaline phosphatase fusion protein (AP-EGF) was used as a substrate, allowing the quantitative assessment of EGF-shedding as alkaline phosphatase activity in the conditioned cell culture medium. Wild-type ADAM12-L or the corresponding catalytic site E351Q mutant was coexpressed with AP-EGF in 293-VnR cells, and ADAM12 protease activity was determined as the ratio of EGF-shedding in cells transfected with wild-type ADAM12-L versus catalytic inactive ADAM12-L. Both N-TIMP-2 and N-TIMP-3 inhibited EGF-shedding in a dose-dependent manner (Fig. 2A). In agreement with our *in vitro* data, an almost complete inhibition of shedding activity was observed at 100 nM N-TIMP-3 treatment, whereas N-TIMP-2 at an equimolar concentration inhibited activity ~40%.

We next tested whether the intriguing ability of the N-TIMP-2– Δ ABloop mutant to selectively inhibit ADAM12 over TACE and MT1-MMP *in vitro* was also observed in the cell-based assay. Because some variation between assays exists, we repeated the N-TIMP-2 titration in parallel with the N-TIMP-2– Δ ABloop experiment to allow for a direct comparison. The N-TIMP-2– Δ ABloop inhibited shedding of AP-EGF to a similar extent to what we observed for wild-type N-TIMP-2 (~65% inhibition at 1 μ M concentration) (Fig. 2B). We also tested N-TIMP-2^{TACE}, which had also exhibited improved inhibitory capacity as compared with wild-type N-TIMP-2 *in vitro*. Although it showed a tendency toward increased inhibitory activity, N-TIMP-2^{TACE} was not statistically significantly different from wild-type N-TIMP-2 (Fig. 2C). The finding that neither N-TIMP-2^{TACE} nor N-TIMP-2– Δ ABloop showed improved inhibitory activity against ADAM12-mediated AP-EGF shedding as compared with wild-type N-TIMP-2 may indicate that the TIMP mutant is titrated by other metalloproteinases expressed by the cells, or alternatively, that the interaction of ADAM12 with the cell-bound AP-EGF substrate modifies the TIMP-interaction. Importantly, however, the N-TIMP-2– Δ ABloop mutant had no effect on PMA-induced AP-HB-EGF shedding, which is mediated by TACE and as expected could be blocked with the TACE

inhibitor TAPI-2 (Fig. 2D). Thus, together these findings confirm the specificity of N-TIMP-2 and N-TIMP-2- Δ ABloop against ADAM12 that we observed *in vitro*.

In conclusion, we have identified an ADAM12-selective inhibitory profile of wild-type and mutant TIMPs, which could possibly be used to discover novel ADAM12 substrates and thereby reveal new biological implications of this protease. For example, the prominent cell-surface protein MT1-MMP is shed from the cell-surface by an unidentified ADAM enzyme [37]. Shedding of MT1-MMP can be inhibited by TIMP-3, to a lesser extent by TIMP-2, and weakly by TIMP-1, thus resembling the inhibitory profile of ADAM12. Moreover, the difference in the inhibitory behaviour of full-length TIMPs, N-TIMPs, and mutant N-TIMPs toward ADAM12, ADAM10, and TACE is encouraging with respect to the design of selective inhibitors. In particular, the data obtained for the TIMP-2- Δ ABloop mutant is of great value, and we hope this mutation in combination with other ADAM12 selective mutations could aid the design of a highly selective ADAM12 inhibitor with future therapeutic applications.

ACKNOWLEDGEMENTS

We thank Drs. Archana Sanjay, Shigeki Higashiyama, and Michael Freeman for kindly providing the 293-VnR cells, alkaline phosphatase-tagged EGF constructs, and HB-EGF constructs, respectively. We thank Dr. Peter Stanley, Cambridge Research Institute for the recombinant ADAM17 ectodomain. We also thank Dr. Reidar Albrechtsen, Department of Biomedical Sciences and BRIC, University of Copenhagen for critical reading of the manuscript and Linda Raab for editorial assistance.

FUNDING

The work was supported by the Danish Medical Research Council, the Danish Cancer Society, and the Friis, Munksholm, Lundbeck, and Novo Nordisk Foundations to MK and UW; NIH grant AR40449 to HN; and BBSRC UK, Cancer Research UK to GM.

REFERENCES

- 1 Kveiborg, M., Albrechtsen, R., Couchman, J. R. and Wewer, U. M. (2008) Cellular roles of ADAM12 in health and disease. *Int. J. Biochem. Cell Biol.* **40**, 1685-1702
- 2 Gilpin, B. J., Loechel, F., Mattei, M. G., Engvall, E., Albrechtsen, R. and Wewer, U. M. (1998) A novel, secreted form of human ADAM 12 (meltrin alpha) provokes myogenesis in vivo. *J. Biol. Chem.* **273**, 157-166
- 3 Blobel, C. P. (2000) Remarkable roles of proteolysis on and beyond the cell surface. *Curr. Opin. Cell Biol.* **12**, 606-612
- 4 Murphy, G. (2008) The ADAMs: signalling scissors in the tumour microenvironment. *Nat. Rev. Cancer.* **8**, 929-941
- 5 Kurisaki, T., Masuda, A., Sudo, K., Sakagami, J., Higashiyama, S., Matsuda, Y., Nagabukuro, A., Tsuji, A., Nabeshima, Y., Asano, M., Iwakura, Y. and Sehara-Fujisawa, A. (2003) Phenotypic analysis of Meltrin alpha (ADAM12)-deficient mice: involvement of Meltrin alpha in adipogenesis and myogenesis. *Mol. Cell. Biol.* **23**, 55-61
- 6 Horiuchi, K., Le Gall, S., Schulte, M., Yamaguchi, T., Reiss, K., Murphy, G., Toyama, Y., Hartmann, D., Saftig, P. and Blobel, C. P. (2007) Substrate selectivity of epidermal growth factor-receptor ligand sheddases and their regulation by phorbol esters and calcium influx. *Mol. Biol. Cell.* **18**, 176-188
- 7 Dyczynska, E., Sun, D., Yi, H., Sehara-Fujisawa, A., Blobel, C. P. and Zolkiewska, A. (2007) Proteolytic processing of delta-like 1 by ADAM proteases. *J. Biol. Chem.* **282**, 436-444
- 8 Ito, N., Nomura, S., Iwase, A., Ito, T., Kikkawa, F., Tsujimoto, M., Ishiura, S. and Mizutani, S. (2004) ADAMs, a disintegrin and metalloproteinases, mediate shedding of oxytocinase. *Biochem. Biophys. Res. Commun.* **314**, 1008-1013
- 9 Loechel, F., Fox, J. W., Murphy, G., Albrechtsen, R. and Wewer, U. M. (2000) ADAM 12-S cleaves IGFBP-3 and IGFBP-5 and is inhibited by TIMP-3. *Biochem. Biophys. Res. Commun.* **278**, 511-515
- 10 Jacobsen, J. and Wewer, U. M. (2009) Targeting ADAM12 in human disease: head, body or tail? *Curr. Pharm. Des.* **15**, 2300-2310
- 11 Fernandez-Catalan, C., Bode, W., Huber, R., Turk, D., Calvete, J. J., Lichte, A., Tschesche, H. and Maskos, K. (1998) Crystal structure of the complex formed by the membrane type 1-matrix metalloproteinase with the tissue inhibitor of metalloproteinases-2, the soluble progelatinase A receptor. *EMBO J.* **17**, 5238-5248
- 12 Wisniewska, M., Goettig, P., Maskos, K., Belouski, E., Winters, D., Hecht, R., Black, R. and Bode, W. (2008) Structural determinants of the ADAM inhibition by TIMP-3: crystal structure of the TACE-N-TIMP-3 complex. *J. Mol. Biol.* **381**, 1307-1319
- 13 Amour, A., Knight, C. G., Webster, A., Slocombe, P. M., Stephens, P. E., Knauper, V., Docherty, A. J. and Murphy, G. (2000) The in vitro activity of ADAM-10 is inhibited by TIMP-1 and TIMP-3. *FEBS Lett.* **473**, 275-279
- 14 Lee, M. H., Maskos, K., Knauper, V., Dodds, P. and Murphy, G. (2002) Mapping and characterization of the functional epitopes of tissue inhibitor of metalloproteinases (TIMP)-3 using TIMP-1 as the scaffold: a new frontier in TIMP engineering. *Protein Sci.* **11**, 2493-2503
- 15 Hu, J., Van den Steen, P. E., Sang, Q. X. and Opdenakker, G. (2007) Matrix metalloproteinase inhibitors as therapy for inflammatory and vascular diseases. *Nat. Rev. Drug Discov.* **6**, 480-498
- 16 Overall, C. M. and Kleifeld, O. (2006) Towards third generation matrix metalloproteinase inhibitors for cancer therapy. *Br. J. Cancer.* **94**, 941-946

- 17 Jacobsen, J., Visse, R., Sorensen, H. P., Enghild, J. J., Brew, K., Wewer, U. M. and Nagase, H. (2008) Catalytic properties of ADAM12 and its domain deletion mutants. *Biochemistry*. **47**, 537-547
- 18 Stautz, D., Sanjay, A., Hansen, M. T., Albrechtsen, R., Wewer, U. M. and Kveiborg, M. (2010) ADAM12 localizes with c-Src to actin-rich structures at the cell periphery and regulates Src kinase activity. *Exp. Cell Res.* **316**, 55-67
- 19 Sundberg, C., Thodeti, C. K., Kveiborg, M., Larsson, C., Parker, P., Albrechtsen, R. and Wewer, U. M. (2004) Regulation of ADAM12 cell-surface expression by protein kinase C epsilon. *J. Biol. Chem.* **279**, 51601-51611
- 20 Wewer, U. M., Morgelin, M., Holck, P., Jacobsen, J., Lydolph, M. C., Johnsen, A. H., Kveiborg, M. and Albrechtsen, R. (2006) ADAM12 is a four-leafed clover: the excised prodomain remains bound to the mature enzyme. *J. Biol. Chem.* **281**, 9418-9422
- 21 Chung, L., Shimokawa, K., Dinakarbandian, D., Grams, F., Fields, G. B. and Nagase, H. (2000) Identification of the (183)RWTNRFREY(191) region as a critical segment of matrix metalloproteinase 1 for the expression of collagenolytic activity. *J. Biol. Chem.* **275**, 29610-29617
- 22 Lee, M. H., Rapti, M. and Murphy, G. (2003) Unveiling the surface epitopes that render tissue inhibitor of metalloproteinase-1 inactive against membrane type 1-matrix metalloproteinase. *J. Biol. Chem.* **278**, 40224-40230
- 23 Milla, M. E., Leesnitzer, M. A., Moss, M. L., Clay, W. C., Carter, H. L., Miller, A. B., Su, J. L., Lambert, M. H., Willard, D. H., Sheeley, D. M., Kost, T. A., Burkhart, W., Moyer, M., Blackburn, R. K., Pahel, G. L., Mitchell, J. L., Hoffman, C. R. and Becherer, J. D. (1999) Specific sequence elements are required for the expression of functional tumor necrosis factor-alpha-converting enzyme (TACE). *J. Biol. Chem.* **274**, 30563-30570
- 24 Huang, W., Suzuki, K., Nagase, H., Arumugam, S., Van Doren, S. R. and Brew, K. (1996) Folding and characterization of the amino-terminal domain of human tissue inhibitor of metalloproteinases-1 (TIMP-1) expressed at high yield in *E. coli*. *FEBS Lett.* **384**, 155-161
- 25 Kashiwagi, M., Tortorella, M., Nagase, H. and Brew, K. (2001) TIMP-3 is a potent inhibitor of aggrecanase 1 (ADAM-TS4) and aggrecanase 2 (ADAM-TS5). *J. Biol. Chem.* **276**, 12501-12504
- 26 Troeberg, L., Tanaka, M., Wait, R., Shi, Y. E., Brew, K. and Nagase, H. (2002) *E. coli* expression of TIMP-4 and comparative kinetic studies with TIMP-1 and TIMP-2: insights into the interactions of TIMPs and matrix metalloproteinase 2 (gelatinase A). *Biochemistry*. **41**, 15025-15035
- 27 Lee, M. H., Rapti, M., Knauper, V. and Murphy, G. (2004) Threonine 98, the pivotal residue of tissue inhibitor of metalloproteinases (TIMP)-1 in metalloproteinase recognition. *J. Biol. Chem.* **279**, 17562-17569
- 28 Lee, M. H., Rapti, M. and Murphy, G. (2004) Delineating the molecular basis of the inactivity of tissue inhibitor of metalloproteinase-2 against tumor necrosis factor-alpha-converting enzyme. *J. Biol. Chem.* **279**, 45121-45129
- 29 Lee, M. H., Rapti, M. and Murphy, G. (2005) Total conversion of tissue inhibitor of metalloproteinase (TIMP) for specific metalloproteinase targeting: fine-tuning TIMP-4 for optimal inhibition of tumor necrosis factor- α -converting enzyme. *J. Biol. Chem.* **280**, 15967-15975
- 30 Moss, M. L. and Rasmussen, F. H. (2007) Fluorescent substrates for the proteinases ADAM17, ADAM10, ADAM8, and ADAM12 useful for high-throughput inhibitor screening. *Anal. Biochem.* **366**, 144-148
- 31 Williams, J. W. and Morrison, J. F. (1979) The kinetics of reversible tight-binding inhibition. *Methods Enzymol.* **63**, 437-467
- 32 Nagase, H., Visse, R. and Murphy, G. (2006) Structure and function of matrix metalloproteinases and TIMPs. *Cardiovasc. Res.* **69**, 562-573

- 33 Lee, M. H., Verma, V., Maskos, K., Becherer, J. D., Knauper, V., Dodds, P., Amour, A. and Murphy, G. (2002) The C-terminal domains of TACE weaken the inhibitory action of N-TIMP-3. *FEBS Lett.* **520**, 102-106
- 34 Rapti, M., Atkinson, S. J., Lee, M. H., Trim, A., Moss, M. and Murphy, G. (2008) The isolated N-terminal domains of TIMP-1 and TIMP-3 are insufficient for ADAM10 inhibition. *Biochem. J.* **411**, 433-439
- 35 Lee, M. H., Verma, V., Maskos, K., Nath, D., Knauper, V., Dodds, P., Amour, A. and Murphy, G. (2002) Engineering N-terminal domain of tissue inhibitor of metalloproteinase (TIMP)-3 to be a better inhibitor against tumour necrosis factor-alpha-converting enzyme. *Biochem. J.* **364**, 227-234
- 36 Maskos, K., Fernandez-Catalan, C., Huber, R., Bourenkov, G. P., Bartunik, H., Ellestad, G. A., Reddy, P., Wolfson, M. F., Rauch, C. T., Castner, B. J., Davis, R., Clarke, H. R., Petersen, M., Fitzner, J. N., Cerretti, D. P., March, C. J., Paxton, R. J., Black, R. A. and Bode, W. (1998) Crystal structure of the catalytic domain of human tumor necrosis factor-alpha-converting enzyme. *Proc. Natl. Acad. Sci. U. S. A.* **95**, 3408-3412
- 37 Toth, M., Sohail, A., Mobashery, S. and Fridman, R. (2006) MT1-MMP shedding involves an ADAM and is independent of its localization in lipid rafts. *Biochem. Biophys. Res. Commun.* **350**, 377-384

FIGURE LEGENDS

Fig. 1: Sequence alignments and cocrystal structure of TACE–N-TIMP-3.

A) The cocrystal structure of the TACE–N-TIMP-3 complex (Protein Data Bank code 3CKI) was visualized using the PyMol molecular viewer tool from LeNovo Scientific (blue ribbon, N-TIMP-3; red ribbon, TACE catalytic domain; purple sphere, catalytic zinc). Key secondary structural elements (strands [s] and helices [h]) and N-TIMP-3 residues are labelled. **B)** Clustal W sequence alignment of ADAM12-Cat and TACE-Cat. Identical residues are highlighted in gray and cysteines in yellow. The secondary structural elements, strands (s) and helices (h), are underlined with arrows and bars, respectively, and the highly conserved Zn²⁺ coordination site is highlighted by the black square. **C)** Sequence alignment of N-TIMP-1–3 using the same colouring code as in B. The N-terminal wedge and the AB-, CD-, and EF-loop regions are highlighted with black squares.

Fig. 2: Effect of TIMPs on cell-based ADAM-mediated ectodomain shedding activity.

A-C) Forty-eight hours after transfection with either wild-type ADAM12-L or the corresponding catalytic site E351Q mutant and AP-EGF, 293-VnR cells were treated with vehicle control (C), wild-type N-TIMP-3 (N-TIMP3), N-TIMP-2 (N-TIMP2), N-TIMP-2 with the AB-loop deleted (N-TIMP2– Δ ABloop), or the N-TIMP-2^{TACE} mutant (N-TIMP2^{TACE}) recombinant protein for 1 h at the indicated concentration (in panel C, a concentration of 0.1 μ M was used). ADAM12-mediated EGF shedding was calculated as alkaline phosphatase activity in the cell media divided by alkaline phosphatase activity in the media plus corresponding cell lysate from cells transfected with AP-EGF and wild-type ADAM12-L relative to cells transfected with AP-EGF and catalytically inactive ADAM12-L (E351Q). **D)** HT1080 cells stably expressing AP-HB-EGF were treated with 400 nM PMA or vehicle control in combination with 0.1 μ M recombinant wild-type N-TIMP-2 (N-TIMP2) or N-TIMP-2 with the AB-loop deleted (N-TIMP2– Δ ABloop) mutant for 30 minutes. The TACE inhibitor TAPI-2 (10 μ M) was used as a positive control. All data are shown as the mean of 3-5 independent experiments, each performed in triplicate, and error bars represent the standard error of the mean. *p<0.05, **p<0.01, ***p<0.005 relative to control-treated cells.

Table 1

Apparent inhibition constants ($K_{i(app)}$, nM) of wild-type TIMPs, N-TIMPs, and N-TIMP mutants against ADAM12

Wild-type full-length and N-terminal forms of N-TIMP-1–3, as well as N-TIMP mutants were tested against ADAM12-S and ADAM12-Cat and compared with inhibition constants for TACE-Cat or the full-length extracellular part of TACE (TACE-long) derived from the literature. The mutants N-TIMP-1^{TACE} (V4S/V69L/T98L/TIMP-3–ABloop) and N-TIMP-2^{TACE} (S2T/A70S/V71L/TIMP-3–ABloop) were originally designed to increase the binding affinity against TACE. AB-loop mutations represent substitutions or deletion of the AB-loop region or a point mutation at position 34 (F34G) in the AB-loop. Data are presented as the mean ($n \geq 3$) \pm S.D.

	ADAM12-Cat	ADAM12-S	TACE-Cat	TACE-long
N-TIMP-1	778 \pm 90	> 500	356 \pm 87 ^[23]	
TIMP-1	741 \pm 62	223 \pm 30		
N-TIMP-2	5.5 \pm 0.7	69.7 \pm 8.8	893 \pm 126 ^[24]	
TIMP-2	2.5 \pm 0.3	84.0 \pm 13.6		
N-TIMP-3	0.93 \pm 0.09	4.4 \pm 0.4	0.22 \pm 0.07 ^[25]	1.75 \pm 0.20 ^[25]
N-TIMP-1^{TACE}	1.9 \pm 0.18	16.4 \pm 2.2	0.14 \pm 0.06 ^[30]	
N-TIMP-2^{TACE}	0.65 \pm 0.02	6.0 \pm 0.6	1.49 \pm 0.31 ^[24]	
N-TIMP-1[V4S]	N/A	122 \pm 12.6	216 \pm 44 ^[23]	
N-TIMP-1[V4A]	N/A	190 \pm 30.7	497 \pm 180 ^[30]	
N-TIMP-1[T98L]	11.2 \pm 2.1	21.7 \pm 2.3	21.1 \pm 4.1 ^[30]	
N-TIMP-2^{TACE}[L100E]	4.1 \pm 0.37	22.0 \pm 2.8	35.9 \pm 3.7 ^[24]	
N-TIMP-1[TIMP-2–ABloop]	247 \pm 65.6	> 500	57.9 \pm 33 ^[30]	
N-TIMP-1[TIMP-3–ABloop]	N/A	66.0 \pm 4.0	67 \pm 17 ^[23]	452 \pm 86 ^[23]
N-TIMP-2^{TACE}[F34G]	N/A	18.0 \pm 2.2	21.6 \pm 2.9 ^[24]	
N-TIMP-2-ΔABloop	2.5 \pm 0.2	28.1 \pm 2.4		> 9000

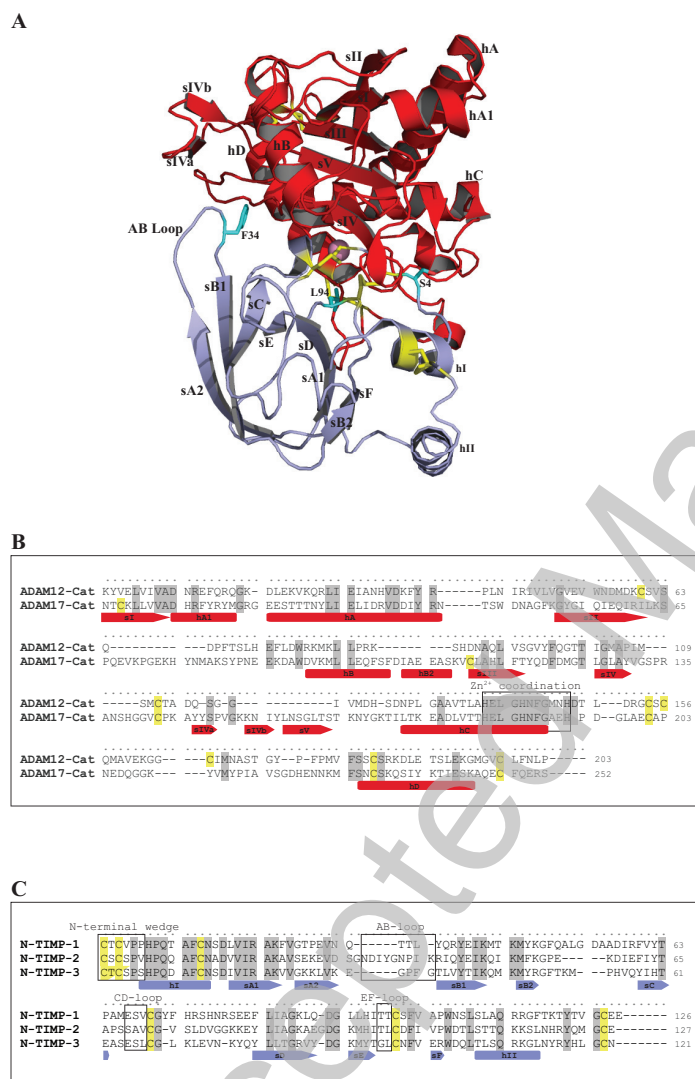


Figure 1

THIS IS NOT THE VERSION OF RECORD - see doi:10.1042/BJ20100649

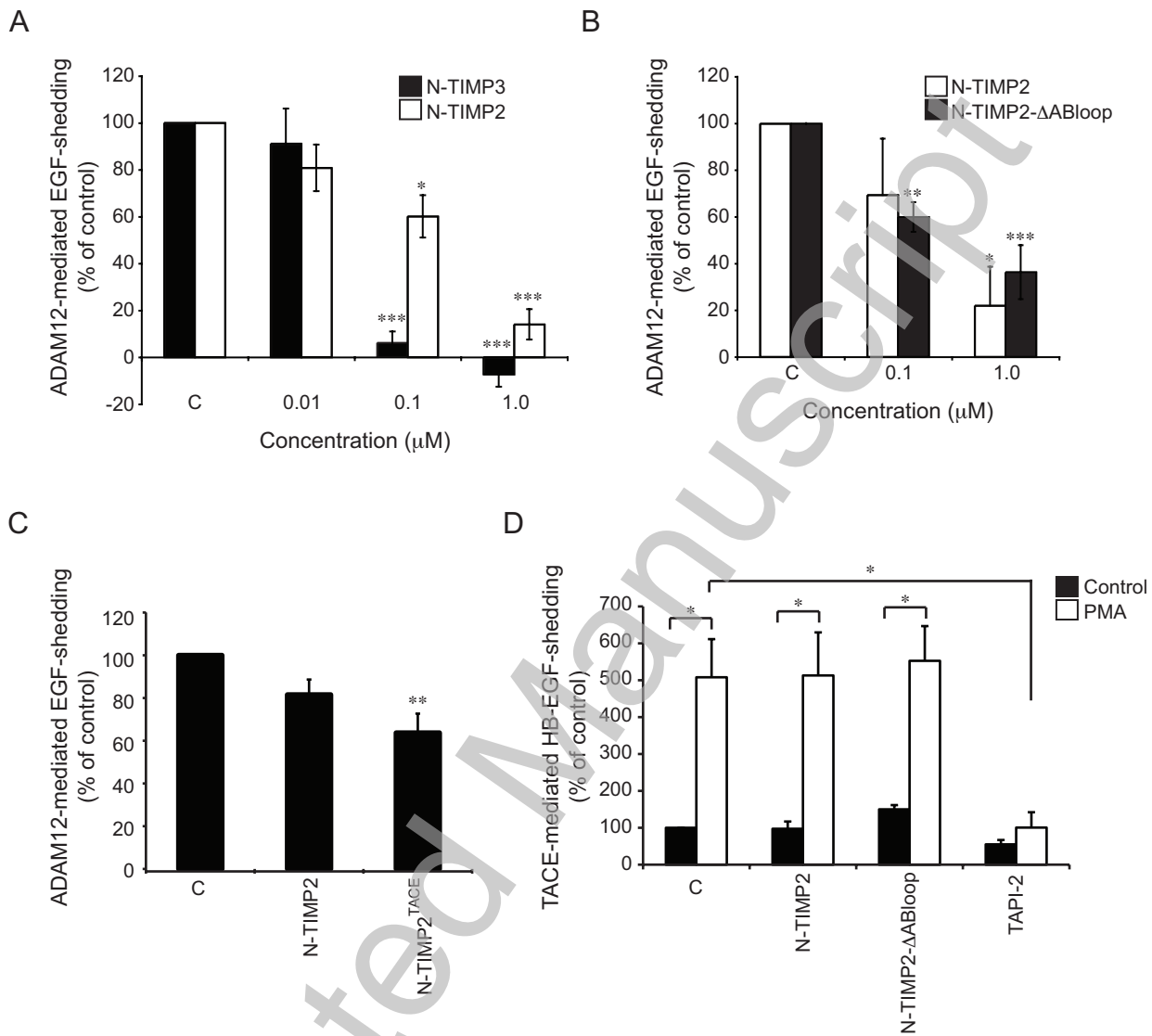


Figure 2